The Journal of Neuroscience, May 1995, 15(5): 3716–3729

Retinal Axon Divergence in the Optic Chiasm: Uncrossed Axons Diverge from Crossed Axons within a Midline Glial Specialization

Riva C. Marcus,[1] Richard Blazeski,[1] Pierre Godement,[2] and Carol A. Mason[1]

[1]Departments of Pathology, and Anatomy and Cell Biology, Center for Neurobiology and Behavior, College of Physicians and Surgeons, Columbia University, New York, New York 10032 and [2]Institut Alfred Fessard, CNRS UPR 2212, 91198 Gif-Sur-Yvette, France

A long-standing question is how fiber pathways in the mammalian CNS project to both sides of the brain. Static and real-time analyses of dye-labeled retinal axons (Godement et al., 1990, 1994) have demonstrated that at embryonic day 15–17 in the mouse, crossed and uncrossed axons from each eye diverge in a zone 100–200 μm proximal to the midline of the optic chiasm. In this study, we identify cellular specializations in this zone that might serve as cues for retinal axon divergence. Second, using growth cone morphology as an indicator of growth cone destination, we analyzed how crossed and uncrossed retinal growth cones related to these cellular components.

Monoclonal antibody RC2, a marker for radial glia in embryonic mouse CNS, revealed a palisade of radial glia straddling the midline. At the midline, a thin raphe of cells that appear morphologically distinct from the radial glia express a free carbohydrate epitope, stage-specific embryonic antigen 1 (SSEA-1). Sections containing DiI-labeled axons and immunolabeled cells indicated that all axons enter the radial glial palisade. Uncrossed axons turn within the palisade, but never beyond the raphe of SSEA-1–positive cells. In addition, ultrastructural analysis indicated that all growth cones contact radial glia, with projections of the growth cone interdigitating with glial fibers. These results demonstrate that retinal axons diverge within a cellular specialization centered around the midline of the developing optic chiasm, consistent with the hypothesis that cues for divergence are located in this zone.

[Key words: retinal axon divergence, midline guidance cues, optic chiasm, SSEA-1, radial glia, RC2]

In mammals, the retina sends a crossed and an uncrossed projection to visual targets in the brain (Polyak, 1957; Guillery, 1982; Chalupa and Lia, 1991; Reese et al., 1991; Baker and Reese, 1993). While it has long been known that the site of retinal axon divergence is the optic chiasm (Guillery, 1982), a classic example of a "decision region," the guidance mechanisms responsible for this bilateral projection are not well understood.

The retinofugal pathway of the embryonic mouse provides a useful model for studies of axon guidance. The topography of the retinal projections (Drager, 1985; Metin et al., 1988) and the origins of retinal ganglion cells that project either ipsi- or contralaterally are known (Godement et al., 1987b, 1990; Colello and Guillery, 1990; Sretavan, 1990). Moreover, our previous studies suggest that in this model system, both positive and negative cues contribute to axon guidance and divergence. Analysis of DiI-labeled retinal axons during the period in which axons forming the crossed and uncrossed projections grow through the chiasm (E15–E17) (Colello and Guillery, 1990; Godement et al., 1990; Sretavan, 1990) showed that uncrossed axons diverge from crossed axons in a zone 100–200 μm proximal to the midline (Godement et al., 1990). Growth cones of uncrossed axons become highly branched or bifurcated in this region, resembling growth cone forms observed *in vitro* at the border of preferred and nonpreferred substrates (Burmeister and Goldberg, 1988) and in decision regions in the nervous systems of different species (e.g., Tosney and Landmesser, 1985; Caudy and Bentley, 1986; Bovolenta and Mason, 1987; Holt, 1989; Norris and Kalil, 1990; Bovolenta and Dodd, 1991; Yaginuma et al., 1991).

The hypothesis that cues for divergence exist in the chiasm is strengthened by observations of retinal axon behavior with video time-lapse microscopy (Sretavan and Reichardt, 1993; Godement et al., 1994). Godement et al. (1994) showed that at E15–E16, all retinal fibers pause for many hours near the midline. Subsequently, whereas growth cones of crossed axons proceed across the midline, growth cones of uncrossed axons become highly complex and turn toward the ipsilateral optic tract. Together, the analysis of retinal axon trajectory in static and living preparations confirmed the hypothesis that growth cone morphology is predictive of growth cone behavior and that crossed and uncrossed axons respond differentially to cues in the chiasm, resulting in progression or inhibition of growth across the midline.

Recent studies have identified non-neuronal specializations at the midline of the vertebrate neuraxis with a role in axon guidance (e.g., Bovolenta and Dodd, 1990; Kuwada et al., 1990; Snow et al., 1990; Jhaveri, 1993). Although retinal axon relationships with non-neuronal cells in their path have been described previously (Silver, 1984; Bovolenta and Mason, 1987; Bovolenta et al., 1987; Guillery and Walsh, 1987; Silver et al.,

Received Sept. 28, 1994; revised Dec. 19, 1994; accepted Dec. 21, 1994.

We are grateful to our colleagues Drs. Jane Dodd, Jonathan Lustgarten, and Li-Chong Wang for critically reading the manuscript and for many encouraging and insightful discussions. We also thank Dr. Jean-Paul Misson for initially providing us with the RC2 antibody and for encouraging these studies. Chung-Liang Chien and Martin Seidensticker participated in the early stages of the analysis of the glial palisade and growth cone relationships, respectively. Support was provided by NIH Grant NS 27615 (Javits Award) (C.A.M.), Program Project NS30532, and NRSA Award F32 EY06510 (R.C.M.) and by NATO Grant 890370 (P.G.).

Correspondence should be addressed to Dr. Carol Mason, Department of Pathology, Columbia University, College of Physicians and Surgeons, 630 West 168th Street, Room 14-509, New York, NY 10032.

1987; Colello and Guillery, 1992), evidence for cellular specializations near the chiasmatic midline was lacking until recent analyses with glial markers (Silver et al., 1993; Reese et al., 1994) and studies of a receptor kinase in midline structures (McKanna and Cohen, 1989; McKanna, 1992).

In this study we looked for cellular specializations in the mouse optic chiasm that would be candidate cues for axon divergence, and used the correlation between growth cone morphology and trajectory to investigate how DiI-labeled retinal axons relate to cellular components of the chiasm. A palisade of radial glia was found straddling the chiasm midline, occupying the zone where axons diverge. All retinal axons enter the palisade and contact radial glial fibers, suggesting that the radial glia may present cues that contribute to retinal axon divergence. In addition, a narrow band of cells expressing stage-specific embryonic antigen 1 (SSEA-1) is situated at the midline itself, further illustrating the specialized cellular organization of this region of the optic chiasm. The demonstration that both crossed and uncrossed axon populations diverge within the zone occupied by these cells, is consistent with the hypothesis that cues that direct retinal axon guidance are located near the midline of the optic chiasm.

Materials and Methods

All experiments were carried out with C57Bl/6J mice derived from a timed-pregnancy breeding colony in this department. The morning on which a plug was found is considered embryonic day 0.

DiI labeling of retinal axons in fixed tissue

Pregnant mothers were anesthetized with ketamine/xylazine, and embryos removed one at a time by cesarean section. Embryos between E15 and E17 were perfused transcardially with 4% paraformaldehyde in 0.1 M Sorensen's phosphate buffer.

Optic axons were labeled with DiI (1,1 -dioctadecyl-3,3,3′,3′-tetramethylindocarbocyanine perchlorate), generally following the procedures in Godement et al. (1987b, 1990). Following fixation, the retina was slit with a fine scalpel and a crystal of DiI was placed in the slit. Brains were stored for 10 d to 2 weeks in buffer with sodium azide at room temperature in the dark. Fibers with a crossed destination were labeled in the areas of retina giving rise to crossed fibers (nasal or dorsal temporal). The majority of preparations analyzed in this study were labeled in ventrotemporal retina. Uncrossed fibers were labeled only when DiI was applied to ventrotemporal retina. Some crossed fibers were also labeled following DiI applications to ventrotemporal retina. These fibers may have originated from outside of the ventrotemporal crescent due to spread of the dye, or from the small population of crossed axons that are intermixed among uncrossed axons in this region of the retina (Colello and Guillery, 1990).

Sectioning. Brains were embedded in agar, cut at 75 μm on a vibratome, and collected in phosphate buffer.

Photooxidation of DiI. In vibratome sections of interest, DiI was photoconverted from a fluorescent compound to a dark brown reaction product by the method of Sandell and Masland (1988). Optimal results were obtained with a Nikon 10× or 20× Neofluor objective and a 100 W mercury lamp, on a Nikon Optiphot microscope. With the 10× objective, the average reaction time was 20–30 min, whereas with the 20× objective, the reaction occurred in 10–15 min.

For light microscopy, sections were mounted on subbed slides, dried, dehydrated in ethanol, cleared in xylene, and coverslipped with Permount.

Immunocytochemistry

Cryostat sections of brains fixed and perfused as for DiI injections were cut at 15–20 μm. Vibratome sections of brains with and without DiI labeling, were cut at 75 μm.

Antibodies. Radial glia were visualized by immunostaining with monoclonal antibody RC2, which specifically stains radial glia in the mouse CNS (Misson et al., 1988). This antisera was originally a gift of Dr. J.-P. Misson and V. Caviness, and subsequently produced by clones provided by Dr. M. Yamamoto and maintained in Dr. T. Jessell's laboratory.

Monoclonal antibody (MAB) 480-1.1, an IgM raised in mouse (Solter and Knowles, 1978), was prepared from cells obtained from the Developmental Studies Hybridoma Bank, by Dr. J. Dodd. This MAB recognizes the stage-specific embryonic antigen 1 (SSEA-1), on early embryonic stem cells as well as human granulocytes (Knowles et al., 1982). The antigen, a lactose series oligosaccharide, is expressed in several regions of the CNS, including radial glia of the spinal cord (Dodd and Jessell, 1985), the floor plate (Dodd, personal communication), and astrocytes in the cerebellum (Lagenaur et al., 1982).

Immunostaining—light microscopy. Sections were first incubated in 10% normal goat serum (NGS) in Tris-buffered saline (TBS), pH 7.2, for 1 hr at room temperature, followed by an overnight incubation in the primary antibodies (1:1 for both MABs RC2 and 480-1.1) in 1% NGS-TBS with 0.1% Triton X-100, at 4°C. Control sections were incubated with preimmune serum. After three washes in buffer, sections were incubated with peroxidase-coupled goat anti-mouse IgM (1:100) for 1 hr at room temperature, and the sections washed thoroughly in buffer. Sections were reacted with diaminobenzidine [10 mg DAB/20 ml 0.05 M Tris (pH 7.6), adding 6.6 μl of H_2O_2] for 10 min, then washed several times with TBS. Sections were mounted on gel-coated slides, allowed to dry, dehydrated, cleared in xylene, and coverslipped with Permount.

Immunostaining of DiI-labeled sections. For double-labeling, vibratome sections with DiI-labeled axons were immunostained after photoconversion. Sections were washed in phosphate buffer at the end of the photoconversion and immediately immunostained by the methods above, with the exception that the DAB reaction product was enhanced with cobalt (Adams, 1980), resulting in a blue-black reaction product that contrasted well with the reddish brown of the photoconverted DiI reaction product.

Immunostaining—electron microscopy. Embryos were perfused with 4% paraformaldehyde and vibratome sections cut at 75 μm. Sections were immunostained with RC2 as described above. Sections of choice were then prepared for electron microscopy as described below. After removing the embedded vibratome section from the plastic slides, thin sections were cut directly.

Electron microscopy of DiI-labeled axons

For electron microscopy of DiI-labeled axons, embryos were perfused as above but with 0.5% glutaraldehyde/2.5% paraformaldehyde in phosphate buffer. Following dye-labeling of retinal axons, vibratome sections were cut at 75 μm and sections of interest were subjected to photoconversion as described above.

Correlative light and electron microscopy was carried out by methods we developed previously for HRP-labeled axons (e.g., Bovolenta and Mason, 1987). Seven-micrometer sections were cut from the original 75 μm section embedded in epon, and photographs and drawings of the two kinds of sections were matched. Selected 7 μm sections were remounted and thin sections were cut, stained, and examined on a JEOL 100S electron microscope. The drawings and photographs of the 75 and 7 μm sections served as guides for relocating specific axons and growth cones.

Analysis

Over 50 preparations were double-labeled with DiI and monoclonal antibody RC2, and seven with DiI and monoclonal antibody 480-1.1 against SSEA-1. These preparations were studied and photographed on a Leitz Orthoplan microscope and Vario-orthomat camera. Sections from five brains single-labeled with RC2, and four preparations containing only DiI-labeled growth cones, were analyzed with the electron microscope.

The relationship of optic axons to the radial glial palisade was analyzed in horizontal sections from seven preparations containing both RC2-immunolabeled cells and DiI-labeled growth cones. First, a camera lucida was used to draw the outlines of the RC2-labeled palisade and the positions of the dye-labeled growth cones. Growth cones were divided into different categories as described in the text. For each drawing, the outline of the palisade was divided into 26 equal sectors, thereby producing a map of the relative position of labeled growth cones with respect to the palisade. These "normalized" growth cone positions were then plotted on a schematic drawing of the RC2-positive palisade in a horizontal section through the brain.

For ultrastructural analysis of dye-labeled growth cones, 10 μm sections were thin-sectioned, resulting in about 100 serial sections. The growth cone of interest was usually visible in 30–70 of the sections. Each section through the growth cone under study was examined, and roughly half of the sections through the growth cone were photographed. Growth cones were scored as to whether they contacted radial glial profiles, the nature of the contact (simple apposition or enwrapping of glial processes by parts of the growth cone), the presence of specialized junctions, and appositions with other axons or cells. Eleven growth cones were studied in this manner.

Results

A radial glial palisade is located at the chiasm midline

Our analyses of DiI labeling in fixed and living preparations of the developing mouse visual system indicate that the uncrossed retinal projection arising from ganglion cells in ventrotemporal retina grows into the chiasm from E15–E17 (see Godement et al., 1994). Uncrossed axons form highly complex, spread growth cones in a zone 100–200 μm lateral to the midline. These shapes develop prior to a turn away from this region back to the ipsilateral optic tract (Godement et al., 1990, 1994). Since previous studies in both invertebrates and vertebrates have implicated glial cells in shaping axon trajectories in the CNS (e.g., Silver, 1984; Jacobs and Goodman, 1989; Norris and Kalil, 1991; Tear et al., 1993), we used the monoclonal antibody RC2, which reveals radial glia in the mouse CNS, to label glia in the developing optic chiasm.

At E15–E17, RC2 immunostaining revealed a dense grouping of radial glia that extends from the floor of the third ventricle to the pial surface of the brain, and which straddles the midline throughout the entire rostrocaudal length of the chiasm. The structure of this radial glial "palisade" was evident in both frontal and horizontal sections through the chiasm (Figs. 1, 2). In the horizontal plane, the RC2-positive radial glial palisade occupied a hexagonal area centered around the midline. At the rostral and caudal ends of the hexagon, the palisade spanned 75 μm on either side of the midline, as measured in frontal sections. Within the rostral tip of the palisade a nest of RC2-negative cells is situated (Fig. 1*A*), corresponding to the "knot" of cells described by Silver by light and electron microscopy (Silver, 1984; Silver et al., 1987; personal communication). At the widest point of the hexagon, the RC2-positive palisade occupied a zone spanning 200 μm to each side of the midline (Figs. 1, 2), corresponding to the region in which uncrossed fibers turn ipsilaterally (see also Godement et al., 1990). The processes of the radial glial palisade arc laterally, leaving the midline between the ventricular zone and the retinal fiber layer relatively free of RC2-positive fibers. Within the retinal fiber layer, RC2-positive endfeet formed a continuous band (e.g., Fig. 1*B*). Caudal to the optic chiasm, RC2-positive fibers fanned out to form an unbroken curtain of fibers (Fig. 1*D*; see also Fig. 8).

When viewed in frontal sections of E15–E16 embryos (Fig. 1*E*), the morphology of the RC2-positive cells matched that of radial glia seen elsewhere in the CNS, having a bipolar morphology and endfeet on the ventral pial surface and in the ventricular lining. Cell bodies of the radial fibers were rarely visualized by RC2 immunostaining because of their scant cytoplasm and small diameter (5–8 μm). When visible, they were positioned along the glial processes above the fiber layer of the chiasm, close to the ventricle. By E17, the radial fibers were more branched at the ventral pole (see Takahashi et al., 1990), with many processes radiating into the fiber stratum. Both crossed and uncrossed growth cones are found ventral to the cell bodies of these radial glia, growing among glial endfeet and processes near the pial surface, in agreement with reports of growth cone location in the chiasm (Guillery and Walsh, 1987; Godement et al., 1990; Reese et al., 1994; Tavendale and Coleman, 1994).

Double labeling of axons and the radial glial palisade

Because the palisade occupies the region within which axons diverge to opposite sides of the brain, we examined the trajectories of both crossed and uncrossed axons with respect to this structure. Horizontal sections were analyzed in which axons were labeled with DiI and photoconverted, and the sections subsequently immunostained for RC2. The results show that the axons of both crossed and uncrossed axons coursed toward the midline, and entered the radial glial palisade (Fig. 2). Uncrossed, turning axons were never seen beyond the midline.

The relationship of individual fibers and growth cones to the RC2-positive cells was analyzed by plotting the trajectory of axons with respect to the glial palisade in camera lucida drawings from sections containing both DiI-labeled axons and immunostained cells. Since we have previously shown that growth cone morphology correlates with behavior and therefore has predictive value (Godement et al., 1990, 1994; Wang et al., 1993), we used growth cone morphology to identify individual fibers as crossed or uncrossed.

Labeled growth cones with *simple* streamlined shapes were divided into three categories. Growth cones that either crossed the midline and were growing on the contralateral side, or those that had turned ipsilaterally and were in or directed to the lateral part of the ipsilateral chiasm comprised the simple "crossed" and "uncrossed" categories, respectively. Growth cones with simple shapes located less than 100 μm proximal to the midline and with the long axis of the growth cone at right angles to the midline were included in the "crossed" category since only growth cones of crossed fibers have such morphologies and orientation this close to the midline (Godement et al., 1994, and see below). Growth cones with simple shapes located more than 100 μm proximal to the midline were classified as "simple-unknown" since growth cones of crossed and uncrossed fibers are intermixed as they grow toward the midline, and therefore could not be identified by position or growth cone form in the lateral chiasm (Colello and Guillery, 1990; Godement et al., 1990, 1994; Sretavan, 1990; Wang et al., 1993).

Growth cones with *complex* spread shapes were divided into two categories. The "turning" category included those growth cones with a branched or Y-shaped base, a filopodium directed back toward the ipsilateral optic tract, and/or with an actual curved or turning profile. These forms were only observed on growth cones of optic axons labeled in ventrotemporal retina, and real-time recordings of turning growth cones confirm that such shapes are seen strictly on uncrossed growth cones preceding a turn back toward the ipsilateral optic tract (Godement et al., 1994). In contrast, growth cones with complex shapes, for example, several filopodia and a typical triangular base but without a Y-shaped base and backward filopodium, have been observed on growth cones of both crossed and uncrossed fibers during the long pauses that they undergo in the midline zone (Godement et al., 1994). Therefore, this second category of complex growth cones were classified as "complex-unknown."

In accordance with the above classification, the relative positions of growth cones in each of the five categories were plotted on a schematic diagram of a horizontal section with respect to the location of the radial glial palisade (Fig. 3). Growth cones of crossing fibers approached the midline in the rostral half of

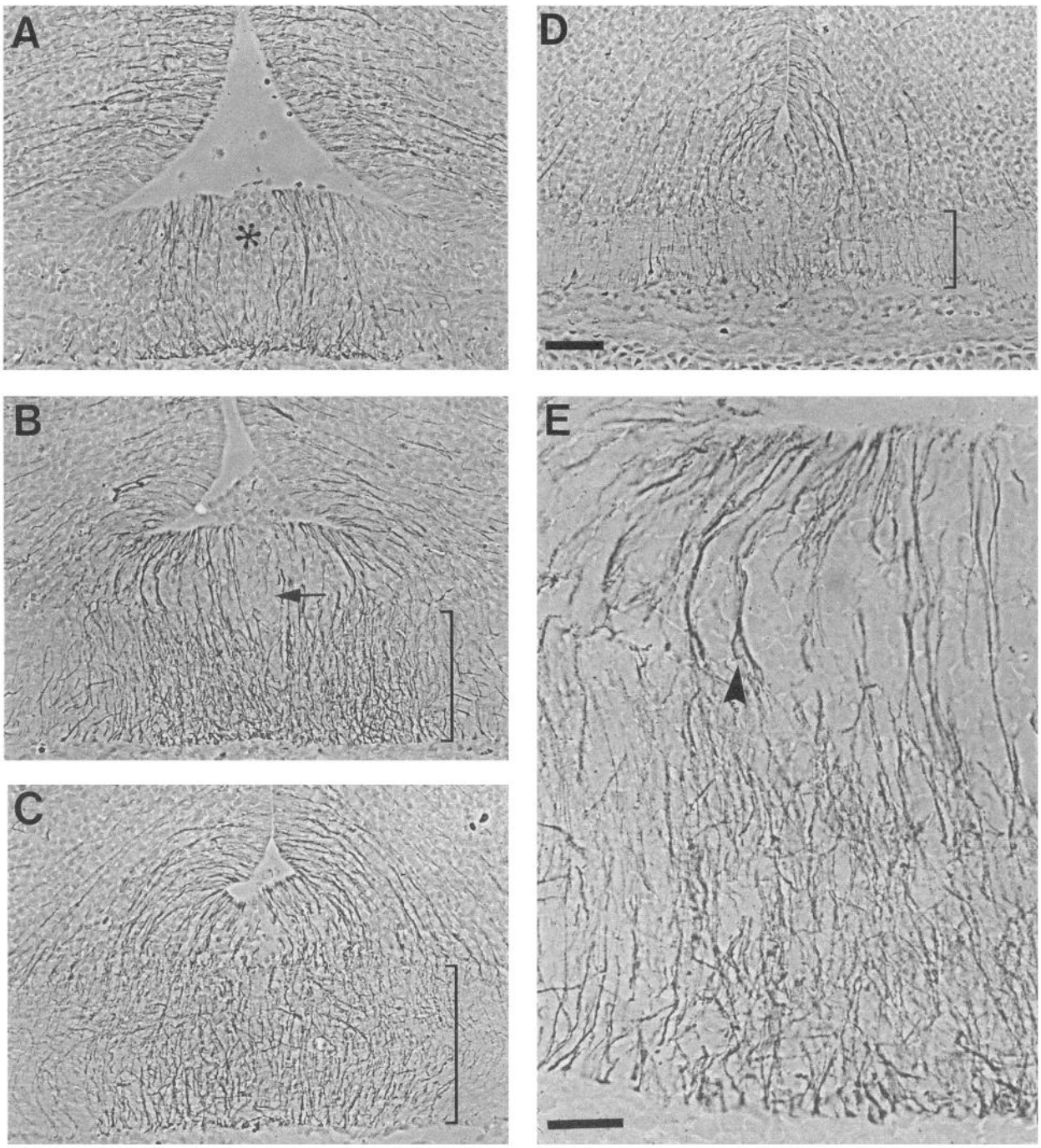

Figure 1. MAB RC2 reveals a palisade of radial glia at the chiasm midline. Cryostat sections through the chiasm of an E16 mouse, cut at 15 μm in the frontal plane, were immunostained with MAB RC2, specific for mouse radial glia. *A*, Section through the rostral chiasm. Radial fibers span the floor of the third ventricle and arch around a cluster of RC2-negative cells, the "glial knot" (*asterisk*; Silver, 1984). *B*, Section 90 μm caudal to *A*. The RC2-positive fibers form a dense palisade on either side of the midline (*arrow*), where labeled cells are scarce. *C*, Section 154 μm caudal to *A*. *D*, Section 165 μm caudal to *A*, through the posterior chiasm. *Brackets in B–D* indicate the retinal fiber layer. *E*, High-power micrograph of palisade in *B*, showing the location of cell bodies above the fiber layer (*arrowhead*). RC2-positive fibers are more highly branched within the stratum of retinal axons. Scale bars: *A–D*, 50 μm; *E* 20 μm.

the chiasm and projected toward the contralateral optic tract, traversing the radial glial palisade on the diagonal (open diamonds). Complex growth cones, that is, those belonging to turning fibers (filled squares) or to growth cones with unknown destination (filled circles), were located primarily within the middle portion of the ipsilateral half of the palisade (see also Fig. 8). Although complex growth cones were found throughout the medial to lateral extent of this area, none were observed contralateral to the midline of the optic chiasm. Once a turn was made, uncrossed fibers and their growth cones (open triangles) grew caudally toward the ipsilateral optic tract on the diagonal, similar to the path taken by crossed fibers subsequent to crossing the midline.

Growth cones were seen near the midline primarily in the

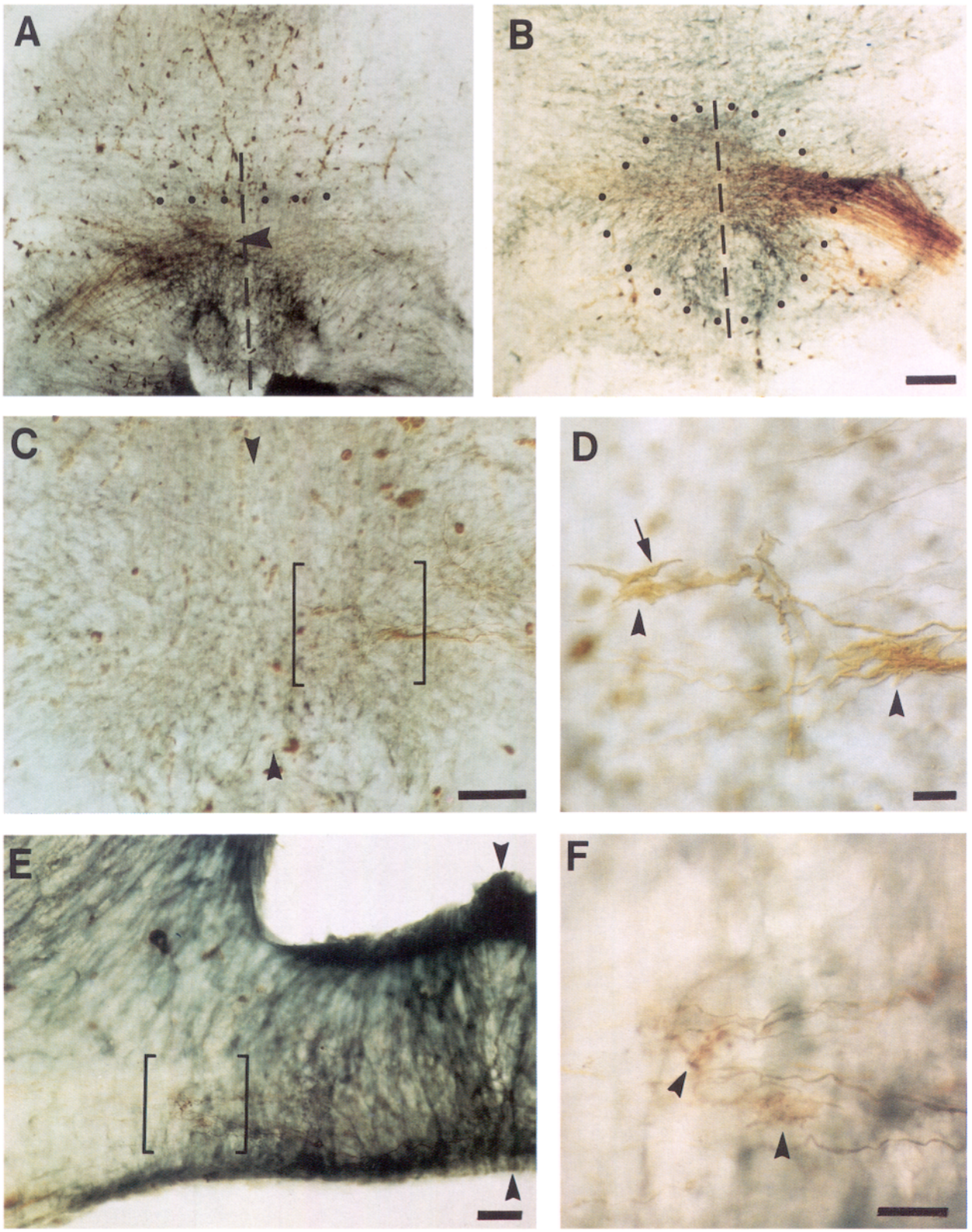

Figure 2. Crossed axons traverse and uncrossed axons turn within the radial glial palisade at the chiasm midline: double-labeled vibratome sections through the chiasm of embryos at E15 containing DiI, photoconverted retinal axons (*brown*), and RC2-labeled cells (*blue-black*). *A–D*, Horizontal sections through the glial palisade. Posterior is at the top of each micrograph. *A*, Turning fibers (indicated by the *arrowhead*) were labeled by applying DiI to ventrotemporal retina. Axons never turn beyond the midline (*dashed line*). *B*, Crossing fibers traverse the glial palisade and splay apart as they cross the midline (*dashed line*). *Dots* outline the "hexagonal-shaped" border of the glial palisade within the chiasm. *C* and *D*, Growth cones of axons labeled in ventrotemporal retina at E16. *C*, *Arrowheads* indicate the midline, and *brackets* denote the area enlarged in *D*. *D*, Complex branched growth cones (*arrowheads*) form within the glial palisade. The left growth cone has a filopodium (*arrow*) directed back (to the right) toward the ipsilateral optic tract. *E* and *F*, Frontal section; complex growth cones are positioned at the lateral edges of the palisade (injection parameters as in *C* and *D*). *E*, Note the lack of RC2 labeling lateral to the palisade, and the decreased staining at the midline (*arrowheads*). *Brackets*

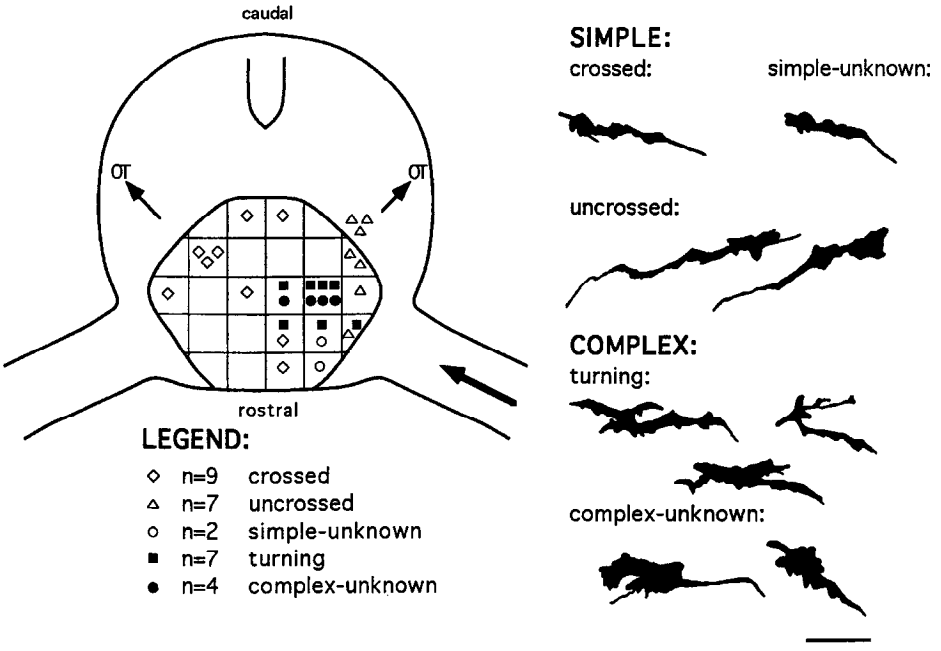

Figure 3. Positions of growth cones with respect to the radial glial palisade. Schematic drawing of a horizontal section through the optic chiasm depicts the relative positions of dye-labeled growth cones with respect to an outline of the radial glial palisade. Labeled axons enter the chiasm from the right optic nerve (*large arrow*). Symbols denote the positions in the chiasm of complex and simple growth cones that are approaching, crossing, or growing away from the midline. Categories of growth cone morphology are as described at the right, in the text, and in Godement et al. (1990, 1994). *Open symbols* represent simple, and *filled symbols*, complex, growth cones, respectively. Scale bar (for camera lucida drawings), 20 μm.

rostral half of the chiasm, reflecting three features of fiber growth. First, growth cones of crossed fibers traverse the midline on the diagonal, such that after crossing, they are positioned in the lateral, caudal reaches of the chiasm. Second, growth cones of uncrossed fibers make their turn within the middle region of the rostrocaudal axis of the palisade and then grow on the diagonal as they course back toward the ipsilateral optic tract. Thus, the trajectories of uncrossed fibers that have completed the turn form a mirror image of those of the crossed fibers, with their growth cones found in the more lateral and caudal regions of the chiasm. Third, as younger contingents of fibers enter the chiasm, they grow rostral to those that have already crossed or turned, and therefore their growth cones are likely to be positioned close to the midline.

One striking aspect of the pattern of turning is that the axons of fibers that completed a turn were positioned nearer to the lateral border of the palisade than fibers bearing growth cones with complex morphologies, prior to or in the act of making a turn. The "bends" that appear 150–200 μm away from the midline might arise if, after approaching the midline, the complex growth cones retract before projecting back to the ipsilateral optic tract. The extensions and retractions of turning growth cones documented with video time-lapse microscopy would account for this feature (see Fig. 8 in Godement et al., 1994). An alternate explanation for this pattern is that uncrossed fibers may turn close to the midline but become displaced laterally as later-arriving fibers approach and turn nearer to the midline. A third possibility is that growth cones tow their axons behind them as they extend into the ipsilateral optic tract, thereby pulling their axon laterally.

Cellular relationships of retinal axon growth cones and fibers of the radial glial palisade

The relationship of crossed and uncrossed axons with respect to the radial glial palisade was further investigated by an ultrastructural analysis of preparations containing dye-labeled growth cones. Prior to this analysis, we identified the midline glial fibers in sections of chiasm immunostained for RC2 by peroxidase labeling and prepared for electron microscopy. In horizontal sections, round profiles of about 0.5 μm in diameter were immunostained. Clusters of three or four linearly arranged glial profiles were regularly spaced and interspersed among unlabeled axons arrayed in a braided pattern (Fig. 4). A similar arrangement of clusters of radial glia oriented perpendicular to tracts has been described elsewhere in the CNS, for example, in the cerebellum and spinal cord (DeBlas, 1984; Bitner et al., 1987; Edwards et al., 1990). The distance between the radial glial clusters averaged 10 μm, similar to that described in the murine cerebral cortex (Gadisseux et al., 1989).

The analysis of sections double labeled with DiI and monoclonal antibody RC2 demonstrated that the growth cones of both crossed and uncrossed axons enter the palisade. We investigated whether these fibers contact cells of the radial glial palisade by analyzing identified dye-labeled growth cones in the electron microscope. As described for the analysis in Figure 3, the morphology of the growth cones has predictive value for behavior and laterality of projection (Godement et al., 1990, 1994; Wang et al., 1993). Radial glia were unlabeled but identified as three or four linearly arranged round profiles based on the dimensions and arrangements of glial fibers observed in immunolabeled material (Fig. 4).

Five growth cones with simple streamlined shapes that were seen by light microscopy to be both near or crossing the midline, were classified as crossing growth cones. All five contacted other unlabeled axons. In addition, four of the five growth cones contacted radial glial profiles at least once along their length. The absence of contacts by the one growth cone was not surprising since this growth cone was in the process of crossing the midline where fewer radial glial fibers are located. Although by

←

denote the area enlarged in *F*. *F*, *Arrowheads* point to two growth cones with complex morphology just within the lateral border of the palisade. Scale bars: *A* and *B*, 100 μm; *C*, 50 μm; *D* and *F*, 10 μm; *E*, 25 μm.

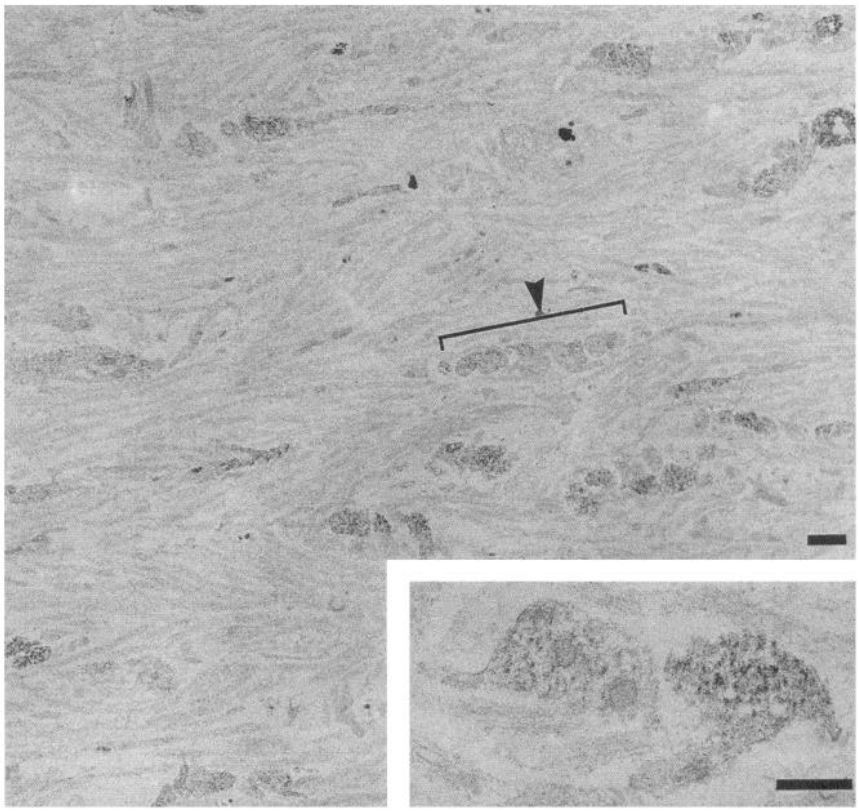

Figure 4. Electron micrograph of a section through the chiasm immunocytochemically stained with MAB RC2. Note the linear groupings of glial fibers cut in horizontal section (*bracket and arrowhead*), and the unlabeled retinal axons running in and among a braided pattern in register with the linear groupings. *Inset* shows higher magnification of two immunostained fibers. Scale bar, 1 μm (*inset*, 0.5 μm).

light microscopy simple growth cones had few filopodia and smooth lamellopodial surfaces, upon ultrastructural examination, small processes were frequently seen to arise from growth cones and wrap around individual glial fibers (Fig. 5*A*).

Seven growth cones with complex morphologies were also examined ultrastructurally. Four of the growth cones were classified as uncrossed using the criteria described above. Three of the growth cones had complex morphologies but without Y-shaped bases or turning profiles (as in Fig. 5*B*), and therefore were considered to belong to either crossed or uncrossed axons. All seven complex growth cones contacted radial glia at multiple sites along the growth cone surface. In individual sections through the major portion of the growth cone under study, the lamellipodia and filopodia extended into and around the clusters of radial glial processes (Fig. 5*B*,*C*), with the result that glial processes were often completely surrounded by a DiI-labeled process.

Because the distance between the linear groupings of radial glia is on the order of 10 μm, the larger complex growth cones, usually broader than 10 μm, would be expected to contact radial glial fibers. In contrast, although this distance is in effect wide enough for simple growth cones (generally 5–8 μm wide) to travel through, they nonetheless also contacted glia. Even though the increased incidence of contact with radial glial fibers by complex growth cones may be predictable because of the size, wide-ranging extent, and appendages extended by these growth cones, the nature of the contacts of the complex uncrossed and crossed growth cones appeared similar to those of the simple growth cones. No membrane specializations such as junctions, or coated vesicles were noted, either in glial processes or in any of the growth cones examined. We cannot rule out, however, that the reaction product from the photoconversion of DiI may have obscured any such structures (see Tavendale and Coleman, 1994).

The ultrastructural data of the cellular relationships of retinal growth cones and radial glial fibers cannot indicate whether radial glial fibers themselves, or other cellular or molecular cues in this locus, present information to the retinal growth cones. Nevertheless, the present data demonstrate that crossed and uncrossed growth cones contact glial fibers of the midline palisade, often quite intimately, before crossing or turning away from the midline, respectively.

A narrow raphe of distinct cells exists at the midline

Because individual growth cones developed complex morphologies well within the radial glial palisade, but never past the midline, we looked for additional cellular specializations nearer the midline. Since the glial palisade is a midline structure putatively involved in axon patterning, and since the ventral midline may be embryologically and cellularly analogous to the floor plate (e.g., Puelles et al., 1987), we screened a number of molecules that are also expressed on immature glia and other midline structures such as the floor plate (Dodd and Jessell, 1985; Dodd, personal communication). One of them, SSEA-1, is expressed on a raphe of cells, 25–50 μm wide and 350 μm long in the rostrocaudal axis, as viewed in the horizontal plane. Caudal to this thin raphe, SSEA-1–positive cells formed a thick band of cells extending mediolaterally (Figs. 6, 7). Rostrally, when viewed in frontal sections, labeled cells with short processes were positioned caudal to the glial knot. Mid-chiasm, a mixture of cells with short processes and cells with radial processes directed toward but not always touching the pial surface demarcated the midline (Fig. 6*B*). The raphe remains narrow through the optic chiasm (Fig. 6*C*) such that at E15–E17, optic

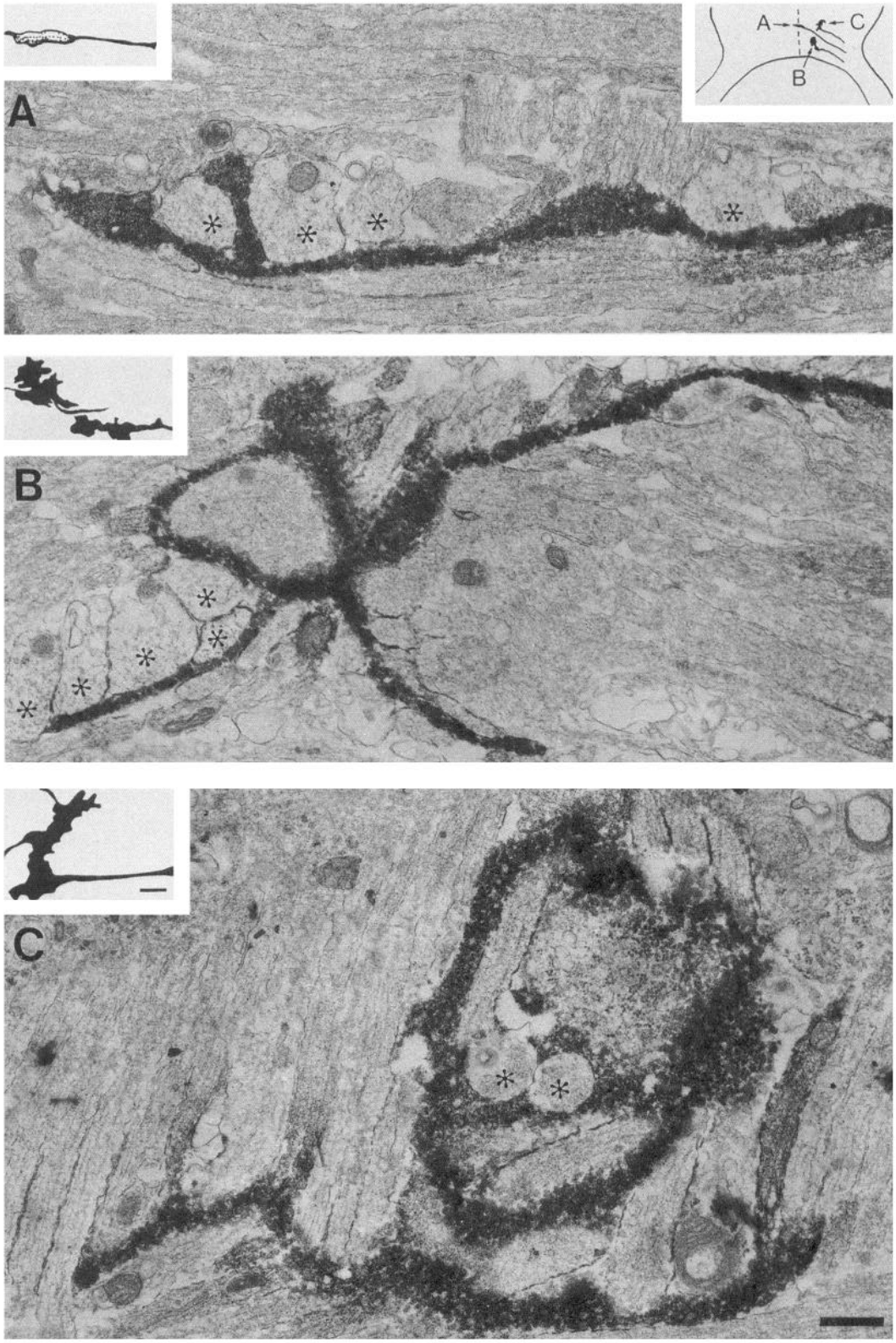

Figure 5. Crossing and turning growth cones relate differently to the glial palisade: electron micrographs of identified axons DiI-labeled in the ventrotemporal retina at E16. Vibratome sections were subsequently photoconverted and processed for electron microscopy. *Inset* shows position of each growth cone and camera lucida drawings show their morphology. *A*, A growth cone crossing the midline. Note that one finger of a lamella of the growth cone interposes between two round clear profiles, identified as radial glial fibers (*asterisks*; see also Fig. 4), but otherwise the body of the growth cone makes simple, continuous contact with the profiles. *B*, A complex growth cone within the glial palisade extends in a bundle of other unlabeled axons. Thin extensions of this growth cone interdigitate with fibers of the radial glial palisade (*asterisks*), as well as other axons. *C*, A complex growth cone in the process of turning away from the midline. The lamellae of this growth cone interpose and surround radial glial fibers (*asterisks*), and contact a grouping of other axons oriented in different axes. Scale bar, 0.5 μm (*insets*, 5 μm).

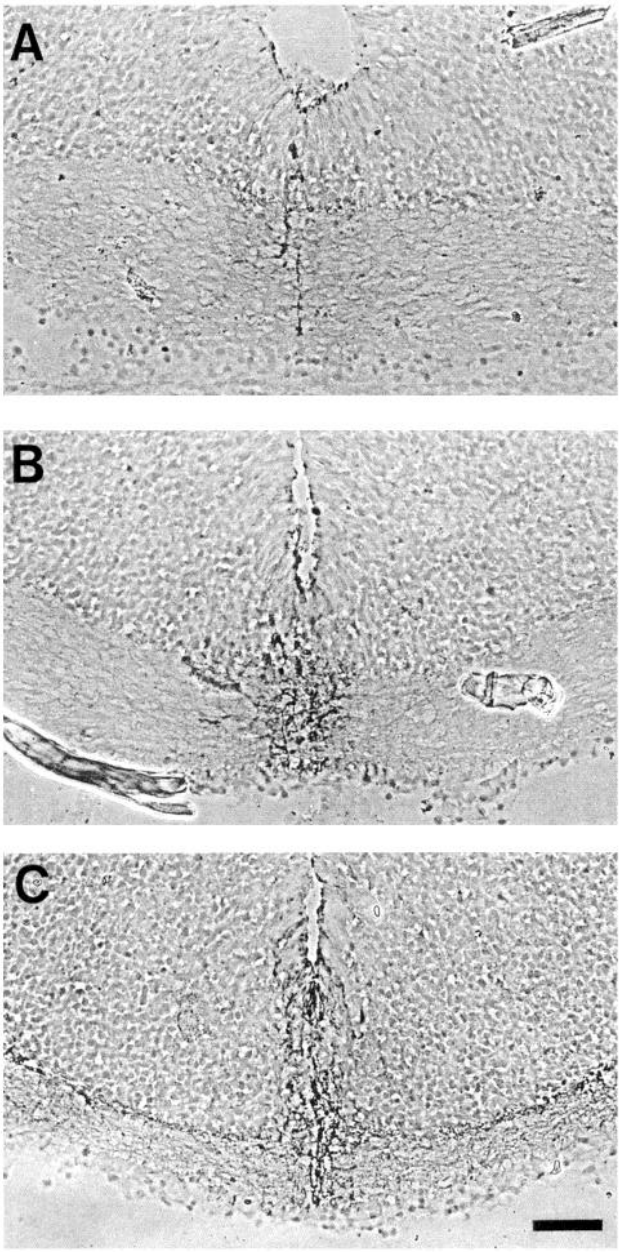

Figure 6. SSEA-1 is expressed in a narrow raphe of cells at the midline. *A–C*, Cryostat sections cut in the frontal plane, moving rostrocaudally through the chiasm from an E15 mouse (compare to Fig. 1). Labeled cells span the entire distance from the third ventricle to the pial surface of the brain, including through the retinal fiber layer. Rostrally (*A*), few radially aligned cells are positioned at the absolute midline. Mid-chiasm (*B*), radial cells and cells with short processes extend 15–25 μm to either side of the midline. Scale bar, 50 μm.

axons are positioned rostral to the broad band of SSEA-1–positive cells but are intersected by the thin raphe of SSEA-1–positive cells at the midline.

To begin to analyze further how growth cones of crossed and uncrossed axons might relate to the SSEA-1–positive cells, we examined horizontal sections containing both DiI-labeled axons and immunolabeled cells (Fig. 7). The midline raphe of SSEA-1–positive cells extended into the chiasm where growth cones of both crossed and uncrossed axons were found. Crossed axons appeared to pass through the SSEA-1–labeled midline, whereas the bends of axons belonging to uncrossed fibers were always located lateral to the midline raphe of cells. Growth cones with complex morphologies, including a backward filopodium and therefore presumed to belong to turning fibers, were also located lateral to this region. Complex growth cones were never located beyond the midline raphe of SSEA-1–positive cells, although they were often positioned up to 50 μm away (see Figs. 2*C*,*D*; 7). Whether growth cones actually contact processes of the SSEA-1–positive cells is currently being analyzed ultrastructurally.

The identity of the cells expressing the SSEA-1 antigen is not known. Since many of the SSEA-1–labeled cells lacked a radial morphology and were concentrated at the midline where RC2-labeled radial glia were sparse (Fig. 1*B*), we conclude that SSEA-1–positive cells are distinct from the RC2-labeled radial glia. We cannot rule out, however, a lineage relationship between cells expressing the antigens recognized by these antibodies.

In summary, two midline specializations were found in the developing optic chiasm. The first is a palisade of radial glia. Retinal axons enter the palisade, contact radial glial fibers, and subsequently diverge. The second is a raphe of cells located at the midline beyond which uncrossed axons do not navigate. These data are consistent with the hypothesis that this specialized zone of the chiasm contains cues that direct retinal axons to project to opposite sides of the brain.

Discussion

This study has demonstrated that within the developing optic chiasm, a specialized cellular arrangement consisting of a palisade of radial glia and a narrow raphe of SSEA-1–positive cells occupies a zone centered around the midline. Growth cones of crossed fibers traverse the glial palisade. Growth cones of uncrossed axons also enter the palisade but turn away from the midline and course back to the ipsilateral optic tract. Turning is therefore coincident with the zone occupied by the radial glia and bounded medially by SSEA-1–positive cells, pointing to this sector of the chiasm as containing cues for divergence. Based on the specialized organization of the chiasm and the paths of diverging retinal axons with respect to this specialization, a model is presented whereby cues from chiasm cells in concert with other cues, such as fiber–fiber interactions, act to shape the trajectories of axons through the optic chiasm.

Cellular organization of the optic chiasm

The present study demonstrates a dense grouping of RC2-positive radial glia flanking the midline in the developing mouse optic chiasm. These results add to the growing list of midline glial specializations identified at the vertebrate neuraxis, for example, in the optic tectum (Barradas et al., 1989; Mori et al., 1990; Jhaveri, 1993), hindbrain (van Hartesveldt et al., 1986; Joosten and Gribnau, 1989; Trevarrow et al., 1990), and spinal cord (Yoshioka and Tanaka, 1989). In agreement with our observations, in the embryonic cat, antibodies against GFAP have revealed glial fibers arching from the floor of the third ventricle to the pia, at the diencephalic/telencephalic border (Silver et al., 1993). In addition, reexamination of sections analyzed in the study by Bovolenta et al. (1987) also revealed a palisade of vimentin-positive cells on either side of the midline, resembling the RC2-positive cells described in the present study (see also Reese et al., 1994, for similar findings in the ferret).

The midline palisade demarcates a change in glial organiza-

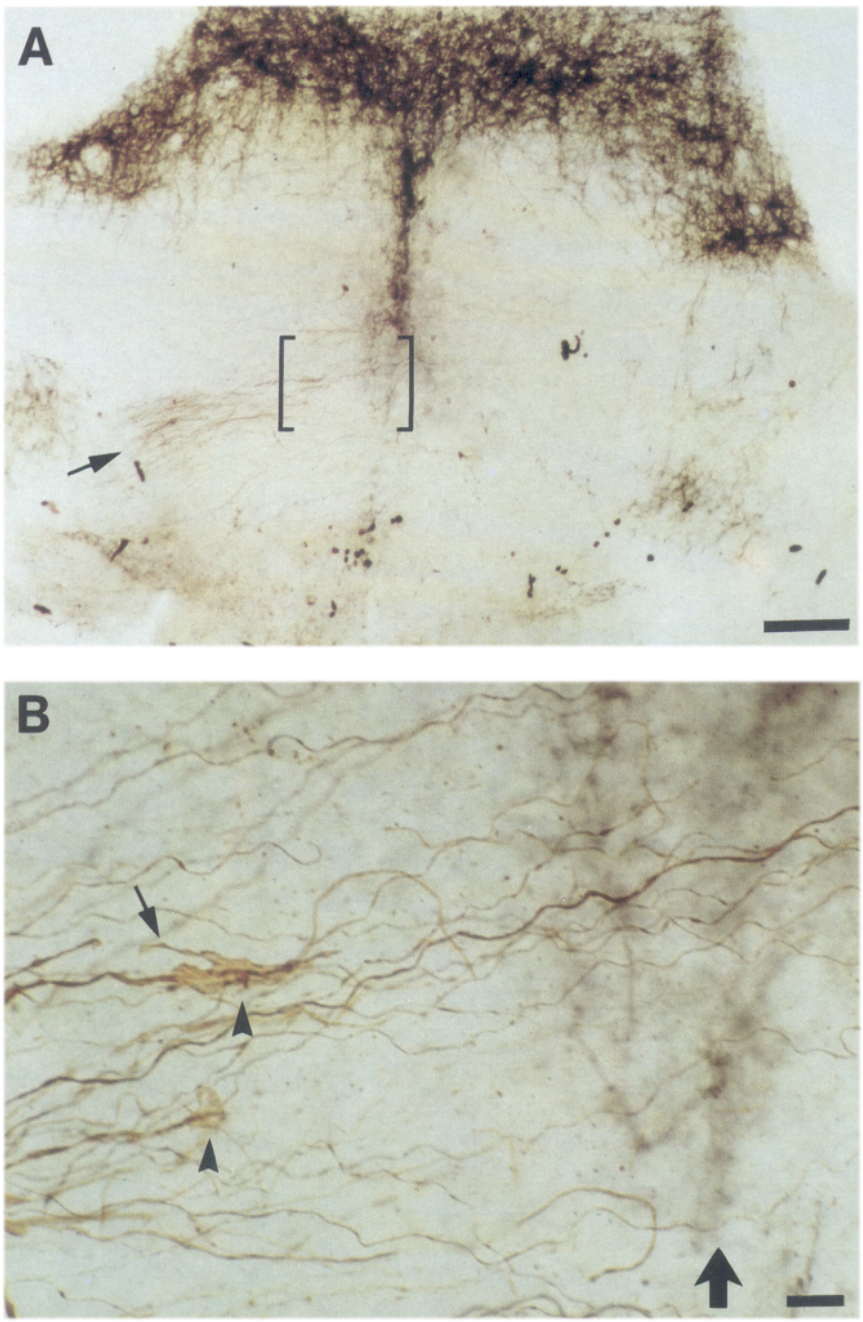

Figure 7. A complex growth cone is near to the raphe of SSEA-1–labeled cells at the chiasm midline: horizontal section through the chiasm of an E15 embryo containing both DiI-photoconverted axons (*brown*) and SSEA-1–labeled cells (*blue-black*). Posterior is up. *A*, A monoclonal antibody to SSEA-1 labels cells in a broad band posterior to the chiasm as well as cells located in a thin raphe at the chiasm midline. DiI was applied to ventrotemporal retina, and the *arrow* indicates labeled axons in the optic nerve. The *brackets* denote the area enlarged in *B*. *B*, *Arrowheads* point to two complex growth cones located proximal to the SSEA-1–labeled cells at the midline (*large arrow*). The upper growth cone has a filopodium (*small arrow*) directed toward the ipsilateral optic tract, common on uncrossed growth cones prior to turning (see Godement et al., 1994). Scale bars: *A*, 100 μm; *B*, 10 μm.

tion in the chiasm, of interest because glial transitions in the visual path have been correlated with changes in fiber arrangement. In the ferret and mouse, a transition from interfascicular glia in the extracranial optic nerve to radial fibers in the intracranial optic nerve and juncture with the lateral chiasm marks a shift of retinal axon growth cones toward the pial surface, thereby effecting an age-related order of optic axons (Guillery and Walsh, 1987; Colello and Guillery, 1992; Reese et al., 1994). In the marsupial, the chiasm has a tripartite structure, with the lateral third of the chiasm demarcated by a ventral fissure. At this point, ipsi- and contralaterally projecting axons separate (Jeffery and Harman, 1992), coincident with the change from interfascicular to radial glia (Taylor and Guillery, 1994).

In addition to the radial glial palisade, cells that appear distinct from RC2-positive cells were revealed by a monoclonal antibody to SSEA-1. As seen in the horizontal plane at E15–E17, these cells form a phalange of cells posterior to the retinal fiber tracts of the chiasm, and extend rostrally as a thin raphe along the midline. With the same antibody to SSEA-1 used in the present study, we have revealed a similar formation of cells at the earliest stages of retinal axon growth (E12.5–E13.5), beneath which retinal axons course as they traverse the chiasm (Marcus and Mason, 1993; unpublished results). In the shape of an arrowhead at this early period, this cell group is remarkably similar to the array of MAP-2–positive cells recently described by Sretavan et al. (1994). We believe that this formation elongates such that by E15–E17, it becomes a thin raphe at the midline and a band of cells positioned caudal to the optic chiasm. The present study demonstrates, however, that unlike axons growing through the chiasm earlier, axons entering the chiasm

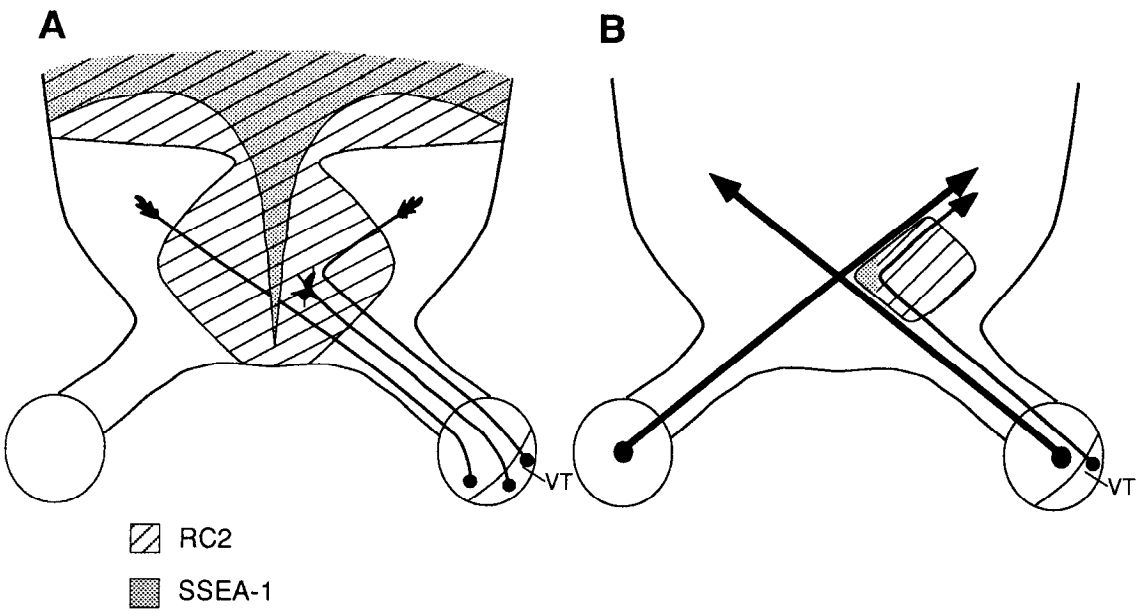

Figure 8. A model for axon growth through the optic chiasm: scheme of the optic chiasm at E15–E17, in horizontal section. The outline of the RC2-expressing glial palisade is *hatched* and the contours of the SSEA-1–expressing cells are *shaded*. *A*, The projection of crossed axons (here shown in nasal retina) and uncrossed axons from ventrotemporal retina is shown with respect to these two cell groupings. *B*, The turning points of uncrossed axons are figured in relation to the crossing axons from each eye, and the two cell groupings figured in *A*. All retinal axons develop complex growth cones and uncrossed axons that develop highly spread, Y-shaped growth cones make turns within a sector of the palisade bounded by the course of the crossing axons from both the ipsilateral and contralateral eyes.

at E15–E17 relate to these cells only if they cross or come close to the midline during the turning process.

Midline specializations: structural and functional similarities with other systems

Radial glia and their endfeet have been implicated as generally preferred substrates for axons in paths (e.g., Silver and Rutishauser, 1984; Hatten et al., 1991) and at the entry to targets (Vanselow et al., 1989; Norris and Kalil, 1991). In contrast, midline structures composed of primitive glia or radial neuroepithelial cells in the CNS of widely separated species have been further implicated as carrying specific cues for axon guidance. In the insect CNS, cells of glial lineage are important for axons crossing the midline (Jacobs and Goodman, 1989; Klambt et al., 1991). The floor plate of the chick and mouse spinal cord acts as a permissive site, serving as an intermediate target for the crossing of the commissural axons (Bovolenta and Dodd, 1990; Yaginuma et al., 1991) and contains tropic cues for attracting axons across the midline (Tessier-Lavigne et al., 1988).

Other midline glial structures, for example, the dorsal roof plate and tectum, appear to play an exclusively inhibitory role (Snow et al., 1990; Wu et al., 1991). In zebrafish, commissural axons traverse the floor plate, whereas other populations are inhibited from entering it (Kuwada et al., 1990; Bernhardt et al., 1992b), a situation more akin to that in the chiasm. Perturbation experiments, using genetic (Bovolenta and Dodd, 1991; Klambt et al., 1991; Bernhardt et al., 1992b; Seeger et al., 1992) or surgical (Wu et al., 1990; Bernhardt et al., 1992a; Jhaveri, 1993) means, have emphasized the importance of midline glial structures to axon patterning.

New work has uncovered antigens expressed by midline cells associated with visual pathways. Radial cells at both the chiasm midline and floor plate in rat express p35 annexin, a calcium- and phospholipid-binding protein, first characterized as a substrate for the EGF receptor tyrosine kinase (McKanna and Cohen, 1989; McKanna, 1992). This epitope is expressed only in the retinal portion of the chiasm and wanes when the small crossing component of ventrotemporal axons grows through the chiasm at the end of the period of retinal axon growth (in rat about E18). Sulfated proteoglycans are located in the roof plate and tectal midline (e.g., Snow et al., 1990; McCabe et al., 1992). Because these molecules can be inhibitory to axonal growth, we are investigating whether sulfated proteoglycans are present at the chiasm midline. Chondroitin sulfate is expressed in the chiasm midline in cells below the ventricle at E15–E17, but is not present within the retinal fiber layer at this time (Lustgarten et al., 1993).

At E12–E14, the MAP-2–positive cells described by Sretavan et al. (1994) express L1, which promotes retinal axon outgrowth, as well as the T-cell antigen CD44, shown to inhibit retinal axon growth *in vitro* (Sretavan et al., 1994). At these earlier ages, a subset of these cells express SSEA-1 (Marcus and Mason, 1993; unpublished results). The relationship between the SSEA-1– and CD44-positive cells at the ages studied in the present analysis is unclear and under investigation. It is unknown whether any of the cells and molecules identified so far in the chiasm midline are relevant for the divergence of optic axons to opposite sides of the brain.

A model for retinal axon divergence

A model for retinal axon divergence is suggested by the present results on localization of cells at the chiasm midline, in combination with previous results on the role of fiber–fiber interactions. Here we show that retinal axons diverge in a region of the chiasm occupied by a cellular specialization composed of radial glia and cells expressing an antigen found on embryonic stem cells. Moreover, the sector of this specialization where uncrossed axons develop complex growth cones and turn is bound-

ed by crossing fibers from each eye, suggesting that a combination of both cellular and axonal cues may play a role directing axons to both sides of the brain.

The findings of the present study highlight cellular specializations at the midline of the optic chiasm. All retinal axonal growth cones contact radial glial fibers of the palisade, and relate intimately to them. The highly complex shapes of growth cones belonging to turning axons and their interdigitating contact with radial glial processes may reflect a response to specific cues on the glial cells, for example, inhibitory molecules that, when recognized by uncrossed axons, block their advance. An alternate possibility is that radial glia do not present specific cues for divergence, and instead may dampen the extension of all retinal axons, regardless of destination. The complex shapes associated with the growth cones of both crossed and uncrossed fibers and the long pauses in extension of all axons (Godement et al., 1994) seen within the area occupied by the glial palisade, is consistent with this possibility. Cues for divergence may in fact derive from other cells in the midline zone. The development of complexity and the increased incidence of contact with radial glia by complex growth cones would therefore not be causal and represent a nonspecific relationship with respect to cues for divergence.

A role for fiber–fiber interactions is suggested if the trajectories of the growth cones, in particular the turning ones on uncrossed fibers, are superimposed on the path of the crossing fibers (Fig. 8). Because uncrossed axons turn in a trigone bordered by crossing fibers, it could be argued that interactions of uncrossed growth cones with other retinal fibers might be sufficient to produce the axon patterning seen during retinal axon divergence. This view is bolstered by other experiments from our laboratory, which show that interactions between fibers from both eyes are important for retinal axon divergence. In animals monocularly enucleated at E13, axons from ventrotemporal retina accumulate in the midline region (Godement et al., 1990; but see Sretavan and Reichardt, 1993). In addition, real-time studies of retinal axon growth in monocularly enucleated animals are in agreement with the static views, indicating that the fibers that normally project ipsilaterally pause for many hours in the midline region, never making the turn or crossing to the opposite optic tract (Godement, unpublished observations). The ultimate behavior of these fibers has not been determined, but previous studies indicate that a reduced ipsilateral component persists into adulthood (Godement et al., 1987a).

In vitro analyses, however, are in agreement with the hypothesis of the present study, that chiasm cells present cues for divergence. Preparations of chiasm membranes (Wizenmann et al., 1993) or monolayers of chiasm midline cells (Guillaume et al., 1991; Wang et al., 1992) preferentially support the growth of crossed axons. Moreover, cell aggregates of isolated chiasm cells, which include the RC2-positive radial glia, inhibit the extension of axons from ventrotemporal retina (Wang et al., 1992 and unpublished). Although neither the *in vitro* analysis nor the present data identify which of the cell types play this role, we propose that interactions with specialized cells of the midline comprise one component of the induction of axon divergence and that interactions with fibers from each retina are another (see also Godement and Mason, 1993). The relative weights of these two components remain to be distinguished by other experimental means.

These studies further advance the hypothesis that interactions of retinal axons with cells of the chiasm midline comprise one step in the establishment of the binocular visual projection. The present findings highlighting a palisade of radial glia and an inner raphe of cells should facilitate identification of the signaling molecules on chiasm components, and in turn, of the distinctions among retinal ganglion cells that underlie their divergence.

References

Adams JC (1980) Heavy metal intensification of DAB-based HRP-reaction product. J Histochem Cytochem 29:775.

Baker GE, Reese BE (1993) Chiasmatic course of temporal retinal axons in the developing ferret. J Comp Neurol 330:95–104.

Barradas PC, Cavalcante LA, Mendez-Otero R, Vieira AM (1989) Astroglial differentiation in the opossum superior colliculus. Glia 2:103–111.

Bernhardt RR, Nguyen N, Kuwada JY (1992a) Growth cone guidance by floor plate cells in the spinal cord of zebrafish embryos. Neuron 8:869–882.

Bernhardt RR, Patel CK, Wilson SW, Kuwada JY (1992b) Axonal trajectories and distribution of GABAergic spinal neurons in wildtype and mutant zebrafish lacking floor plate cells. J Comp Neurol 326:263–272.

Bitner C, Benjelloun-Touimi S, Dupouey P (1987) Palisading pattern of subpial astroglial processes in the adult rodent brain: relationship between the glial palisading pattern and the axonal and astroglial organization. Dev Brain Res 37:167–178.

Bovolenta P, Dodd J (1990) Guidance of commissural growth cones at the floor plate in embryonic rat spinal cord. Development 109:435–438.

Bovolenta P, Dodd J (1991) Perturbation of neuronal differentiation and axon guidance in the spinal cord of mouse embryos lacking a floor plate: analysis of Danforth's short-tail mutation. Development 113: 625–639.

Bovolenta P, Mason CA (1987) Growth cone morphology varies with position in the developing mouse visual pathway from retina to first targets. J Neurosci 7:1447–1460.

Bovolenta P, Liem RKH, Mason CA (1987) Onset of glial filament protein expression and development of astroglial shape in the mouse retinal axon pathway. Dev Brain Res 33:113–126.

Burmeister DW, Goldberg DJ (1988) Micropruning: the mechanism of turning of *Aplysia* growth cones at substrate borders *in vitro*. J Neurosci 8:3151–3159.

Caudy M, Bentley D (1986) Pioneer growth cone morphologies reveal proximal increases in substrate affinity. J Neurosci 6:364–379.

Chalupa LM, Lia B (1991) The nasotemporal division of retinal ganglion cells with crossed and uncrossed projections in the fetal rhesus monkey. J Neurosci 11:191–202.

Colello RJ, Guillery RW (1990) The early development of retinal ganglion cells with uncrossed axons in the mouse: retinal position and axon course. Development 108:515–523.

Colello RJ, Guillery RW (1992) Observations on the early development of the optic nerve and tract of the mouse. J Comp Neurol 317:357–378.

DeBlas AL (1984) Monoclonal antibodies to specific astroglial and neuronal antigens reveal the cytoarchitecture of the Bergmann glia fibers in the cerebellum. J Neurosci 4:265–273.

Dodd J, Jessell TM (1985) Lactoscrics carbohydrates specify subsets of dorsal root ganglion neurons projecting to the superficial dorsal horn of rat spinal cord. J Neurosci 5:3278–3294.

Drager UC (1985) Birth dates of retinal ganglion cells giving rise to the crossed and uncrossed optic projections in the mouse. Proc R Soc Lond [Biol] 224:57–77.

Edwards MA, Yamamoto M, Caviness VSJ (1990) Organization of radial glia and related cells in the developing murine CNS. Neuroscience 36: 121–144.

Gadisseux J-F, Evrard P, Misson J-P, Caviness VSJ (1989) Dynamic structure of the radial glial fiber system of the developing murine cerebral wall: an immunocytochemical analysis. Dev Brain Res 50:55–67.

Godement P, Mason CA (1993) Guidance of retinal fibers in the optic chiasm. Perspect Dev Neurobiol 1:217–225.

Godement P, Salaun J, Metin C (1987a) Fate of uncrossed retinal projections following early or late prenatal monocular enucleation in the mouse. J Comp Neurol 255:97–109.

Godement P, Vanselow J, Thanos S, Bonhoeffer F (1987b) A study in

developing visual systems with a new method of staining neurones and their processes in fixed tissue. Development 101:697–713.
Godement P, Salaun J, Mason CA (1990) Retinal axon pathfinding in the optic chiasm: divergence of crossed and uncrossed fibers. Neuron 5:173–196.
Godement P, Wang L-C, Mason CA (1994) Retinal axon divergence in the optic chiasm: behavior and cues at the midline. J Neurosci 14: 7024–7039.
Guillaume R, Wang L-C, Mason CA, Godement P (1991) Retinal axon-optic chiasm cellular interactions *in vitro*. Soc Neurosci Abstr 17:40.
Guillery RW (1982) The optic chiasm of the vertebrate brain. Contrib Sensory Physiol 7:39–73.
Guillery RW, Walsh C (1987) Changing glial organization relates to changing fiber order in the developing optic nerve of ferrets. J Comp Neurol 265:203–217.
Hatten ME, Fishell G, Stitt T, Mason CA (1991) Glia as a scaffold for development of the CNS. In: Neuroscience research symposium: cell and molecular biology of glia (Mirsky R, Jessen KR, eds), pp 455–465. New York: Saunders.
Holt CE (1989) A single-cell analysis of early retinal ganglion cell differentiation in *Xenopus*: from soma to axon tip. J Neurosci 9:2402–2411.
Jacobs J, Goodman CS (1989) Embryonic development of axon pathways in the *Drosophila* CNS. I. A glial scaffold appears before the first growth cones. J Neurosci 9:2402–2411.
Jeffery G, Harman AM (1992) Distinctive patterns of organisation in the retinofugal pathway of a marsupial. II. Optic chiasm. J Comp Neurol 325:57–67.
Jhaveri S (1993) The midline glia of the tectum: a barrier for developing retinal axons. Perspect Dev Neurobiol 1:237–243.
Joosten EAJ, Gribnau AAM (1989) Astrocytes and guidance of outgrowing corticospinal tract axons in the rat. An immunocytochemical study using anti-vimentin and anti-glial fibrillary acidic protein. Neuroscience 31:439–452.
Klambt C, Jacobs JR, Goodman CS (1991) The midline of the *Drosophila* central nervous system: a model for the genetic analysis of cell fate, cell migration, and growth cone guidance. Cell 64:801–815.
Knowles BB, Rappaport J, Solter D (1982) Murine embryonic antigen (SSEA-1) is expressed on human cells and structurally related human blood group antigen I is expressed on mouse embryos. Dev Biol 93: 54–58.
Kuwada JY, Bernhardt RR, Chitnis AB (1990) Pathfinding by identified growth cones in the spinal cord of zebrafish embryos. J Neurosci 10: 1299–1308.
Lagenaur C, Schachner M, Solter D, Knowles B (1982) Monoclonal antibody against SSEA-1 is specific for a subpopulation of astrocytes in mouse cerebellum. Neurosci Lett 31:181–184.
Lustgarten JH, Marcus RC, Wang L-C, Mason CA (1993) Chondroitin sulfate is localized at the midline during retinal axon divergence in the mouse optic chiasm. Soc Neurosci Abstr 19:1481.
Marcus RC, Mason CA (1993) Early retinal axon growth in the mouse ventral diencephalon. Soc Neurosci Abstr 19:1481.
McCabe CF, Thompson RP, Cole GJ (1992) Distribution of the novel developmentally-regulated protein EAP-300 in the embryonic nervous system. Dev Brain Res 66:11–23.
McKanna JA (1992) Optic chiasm and infundibular decussation sites in the developing rat diencephalon are defined by glial raphes expressing p35 (lipocortin 1, annexin I). Dev Dynam 195:75–86.
McKanna JA, Cohen S (1989) The EGF receptor kinase substrate p35 in the floor plate of the embryonic rat CNS. Science 243:1477–1479.
Metin C, Godement P, Imbert M (1988) The primary visual cortex of the mouse: receptive field properties and functional organization. Exp Brain Res 69:594–612.
Misson J-P, Edwards MA, Yamamoto M, Caviness VS (1988) Identification of radial glial cells within the developing murine cerebral wall: studies based upon a new histochemical marker. Dev Brain Res 44: 95–108.
Mori K, Ikeda J, Hayaishi O (1990) Monoclonal antibody R2D5 reveals midsagittal radial glial system in postnatally developing and adult brainstem. Proc Natl Acad Sci USA 87:5489–5493.
Norris CR, Kalil K (1990) Morphology and cellular interactions of growth cones in the developing corpus callosum. J Comp Neurol 293: 268–281.
Norris CR, Kalil K (1991) Guidance of callosal axons by radial glia in the developing cerebral cortex. J Neurosci 11:3481–3492.
Puelles L, Amat JA, Martinez-de-Torre M (1987) Segment-related, mosaic neurogenetic pattern in the forebrain and mesencephalon of early chick embryos. I. Topography of AChE-positive neuroblasts up to stage HH18. J Comp Neurol 266:247–268.
Reese BE, Guillery RW, Marzi CA, Tassinari G (1991) Position of axons in the cat's optic tract in relation to their retinal origin and chiasmatic pathway. J Comp Neurol 306:539–553.
Reese BE, Maynard TM, Hocking DR (1994) Glial domains and axonal reordering in the chiasmatic region of the developing ferret. J Comp Neurol 349:303–324.
Sandell JH, Masland RH (1988) Photoconversion of some fluorescent markers to a diaminobenzidine product. J Histochem Cytochem 36: 555–559.
Seeger MA, Tear G, Ferres-Marco D, Goodman CS (1992) Mutations affecting growth cone guidance in *Drosophila*. Genes necessary for guidance toward or away from the midline. Neuron 10:409–426.
Silver J (1984) Studies on the factors that govern directionality of axonal growth in the embryonic optic nerve and at the chiasm of mice. J Comp Neurol 223:238–251.
Silver J, Rutishauser U (1984) Guidance of optic axons *in vivo* by a preformed adhesive pathway on neuroepithelial endfeet. Dev Biol 106: 485–499.
Silver J, Poston M, Rutishauser U (1987) Axon pathway boundaries in the developing brain. I. Cellular and molecular determinants that separate the optic and olfactory projections. J Neurosci 7:2264–2272.
Silver J, Edwards MA, Levitt P (1993) Immunocytochemical demonstration of early appearing astroglial structures that form boundaries and pathways along axon tracts in the fetal brain. J Comp Neurol 328: 415–436.
Snow DM, Steindler DA, Silver J (1990) Molecular and cellular characterization of the glial roof plate of the spinal cord and optic tectum: a possible role for a proteoglycan in the development of an axon barrier. Dev Biol 138:359–376.
Solter D, Knowles BB (1978) Monoclonal antibody defining a stage-specific mouse embryonic antigen (SSEA-1). Proc Natl Acad Sci USA 75:5565–5569.
Sretavan DW (1990) Specific routing of retinal ganglion cell axons at the mammalian optic chiasm during embryonic development. J Neurosci 10:1995–2007.
Sretavan DW, Reichardt LF (1993) Time-lapse video analysis of retinal ganglion cell axon pathfinding at the mammalian optic chiasm: growth cone guidance using intrinsic chiasm cues. Neuron 10:761–777.
Sretavan DW, Feng L, Pure E, Reichardt LF (1994) Embryonic neurons of the developing optic chiasm express L1 and CD44, cell surface molecules with opposing effects on retinal axon growth. Neuron 12: 957–975.
Takahashi R, Misson J-P, Caviness VSJ (1990) Glial process elongation and branching in the developing murine neocortex: a qualitative and quantitative immunohistochemical analysis. J Comp Neurol 302:15–28.
Tavendale SJ, Coleman L-A (1994) A study of the microenvironment in the embryonic mouse optic chiasm. Soc Neurosci Abstr 20:1085.
Taylor JSH, Guillery RW (1994) Early development of the optic chiasm in the gray short-tailed opossum, *Monodelphis domestica*. J Comp Neurol 350:109–121.
Tear G, Seeger M, Goodman CS (1993) To cross or not to cross: a genetic analysis of guidance at the midline. Perspect Dev Neurobiol 1:183–194.
Tessier-Lavigne M, Placzek M, Lumsden AGS, Dodd J, Jessell TM (1988) Chemotropic guidance of developing axons in the mammalian central nervous system. Nature 336:775–758.
Tosney KW, Landmesser LT (1985) Growth cone morphology and trajectory in the lumbosacral region of the chick embryo. J Neurosci 5:2345–2358.
Trevarrow B, Marks DL, Kimmel CB (1990) Organization of hindbrain segments in the zebrafish embryo. Neuron 4:669–679.
van Hartesveldt C, Moore B, Hartman BK (1986) Transient midline raphe glial structure in the developing rat. J Comp Neurol 253:175–184.
Vanselow J, Thanos S, Godement P, Henke-Fahle S, Bonhoeffer F (1989) Spatial arrangement of radial glia and ingrowing retinal axons in the chick optic tectum during development. Dev Brain Res 45:15–27.
Wang L-C, Godement P, Mason CA (1992) Cells of the optic chiasm midline inhibit uncrossed retinal fiber outgrowth *in vitro*. Soc Neurosci Abstr 18:222.

Wang L-C, Godement P, Mason CA (1993) Growth cone form is behavior- and position-specific. Soc Neurosci Abstr 19:620.

Wizenmann A, Thanos S, Boxberg Yv, Bonhoeffer F (1993) Differential reaction of crossing and non-crossing rat retinal axons on cell membrane preparations from the chiasm midline: an *in vitro* study. Development 117:725–735.

Wu D-Y, Schneider GE, Jhaveri S (1990) Retinotectal axons cross to the wrong side following disruption of tectal midline cells in the hamster. Soc Neurosci Abstr 16:336.

Wu D-Y, Silver J, Schneider GE, Jhaveri S (1991) The barrier function of tectal midline glial cells and its association with proteoglycan distribution. Soc Neurosci Abstr 17:740.

Yaginuma H, Shunsaku H, Kunzi R, Oppenheim RW (1991) Pathfinding by growth cones of commissural interneurons in the chick embryo spinal cord: a light and electron microscopic study. J Comp Neurol 304:78–102.

Yoshioka T, Tanaka O (1989) Ultrastructural and cytochemical characterisation of the floor plate ependyma of the developing rat spinal cord. J Anat 165:87–100.